194. Conformational Parameters of the Sandalwood-Odor Activity: Conformational Calculations on Sandalwood Odor[1])

by **Gerhard Buchbauer*, Alexander Hillisch, Karin Mraz,** and **Peter Wolschann***

Institut für Pharmazeutische Chemie und
Institut für Theoretische Chemie und Strahlenchemie der Universität Wien,
Althanstrasse 14 and Währinger Strasse 38, A-1090 Wien

Dedicated to Dr. *G. Ohloff* on the occasion of his 70th birthday

(28.IX.94)

The conformational parameters responsible for sandalwood odor were investigated by the 'active-analog approach'. The pharmacophoric (osmophoric) pattern of sandalwood-odor molecules can be outlined as three points: the OH group (point P1), a lipophilic group (point P2) 2.9–3.0 Å distant from the OH group, and a bulky rigid group (point P3), represented as a dummy atom in the middle of the alicyclic system (norbornane bicycle or cyclopentene ring) or a quaternary C-atom. This concept was tested on a series of representative sandalwood-odor compounds and on some structurally similar, but odorless substances.

1. Introduction. – The explanation of structure-activity relationships without the knowledge of detailed information about the three-dimensional structure of the receptor site is a widespread problem. Many methods, *e.g.* molecular dynamics or Monte-Carlo procedures, were applied to many systems of biological interest. But especially the inherent flexible nature of many active molecules is a strong limitation for a general application of such methods, due to extreme large calculation times. Therefore, the concept of constrained conformational search postulating distinct pharmacophors is a common tool in computer-assisted drug design [2]. In particular, the 'active-analog approach' [3–6] appeared as a convenient method, using systematic conformational search [3] [5] to generate a set of energetically allowed conformations based on a grid search of the torsion angles. The aim of this method is the determination of the pharmacophoric pattern of a number of biologically active molecules with different structural properties.

The 'active-analog approach' seems to be especially useful for computer-assisted fragrance design, because no information about the odor-molecule recognition or the structure of the fragrance receptor is known so far. Nevertheless, a large number of structurally different molecules with identical odor impressions were studied from different classes of fragrances, *e.g.* the group of sandalwood-odor substances. More than 100 natural as well as synthetic compounds show the typical warm and woody scent of sandalwood oil [7] [8]. Molecular-similarity studies were performed on sandalwood-odor compounds, using special methods calculating comparable molecular surfaces [9]. In

[1]) Part X; for part IX, see [1].

particular, stereoisomers and optical isomers were investigated [10–15]. In continuation of these studies, the method of 'active-analog approach' was applied to a broad spectrum of different types of sandalwood-odor molecules in order to create a concrete osmophore model for this scent.

2. Compounds. – From different groups of sandalwood-odor molecules, the 12 known structures **A**–**L** (*Fig. 1*) were selected and analyzed by 'active-analog approach' procedures, together with 6 similar, but odorless compounds.

From the literature, the odor of enantiomers is known only in the case of some of these compounds (**A**, **I**). The fragrance of the alcohols **B**–**D** was described for the racemates. Compounds **E**–**K** (exclusive **I**) were diastereoisomer mixtures, no further information about the absolute configuration and selectivity of the odor impression was given. A correlation of the sandalwood odor and the exact 3D structure was described for compounds **A** and **I**, all other compounds were olfactively evaluated as isomer mixtures. From earlier studies [16], it was postulated that in these mixtures only the isomers with largest similarity to the rigid standard molecule **A** possess strongest sandalwood odor, whereas the other isomers show a much weaker odor impression or even no sandalwood scent. The comparison of these isomers with **A** was performed on the base of comparable molecular surfaces [9], and the similarity postulate was found to be valid, *e.g.*, for the explanation of the odor difference of the optical isomers of β-santalol [14]. The most rigid compound 6α-(*tert*-butyl)-*trans*-perhydronaphthalen-2α-ol (**A**) [17] [18] is generally defined as reference molecule for sandalwood odor. This molecule has only two free single bonds: the rotation of the *t*-Bu group leads to identical conformations and the rotation of the C–O bond does not change the heavy-atom skeleton; consequently the molecule exists in only one conformation. Starting from this rather rigid molecule **A**, compounds with increasing flexibility, caused by rotations about C–C single bonds, were taken for the study. A very limited number of conformations are possible for compounds **B** and **C** [19], due to the free rotation of only one C–C single bond and the energetically unfavorable cyclohexane ring inversion. The same free rotation around one single bond occurs in compound **D** [20] [21], but here the ring inversion contributes to a thermodynamic equilibrium. In compounds **E**–**L** [22–29], the number of possible conformations is increased, caused by two single bonds and a flexible cyclopentenyl ring in **E** to the extremely flexible chain of compound **L**.

3. Method of Calculation. – The calculation were accomplished by the program package SYBYL [30] on a *Sun-Sparc-10* workstation. Molecular geometries were built from standard fragments in SYBYL. A global conformational analysis was performed with RANDOMSEARCH [31] and systematic SEARCH [32] (MAXIMIN force field [33]). The hyperspace of the resulting low-energy conformations was investigated for common spatial pharmacophoric orientations. This analysis was performed with the SEARCH program [31] in SYBYL. The parameters used in SEARCH [31] for filtering were: increment for dihedral angle variation; 10°; *van der Waals* radii scaling factors, generally 0.89; 1–4 interaction, 0.85 and 0.65 (for interactions between H-atoms); *E*-window, 10 kcal/mol; grid size for distance map, 0.1 Å; reference conformation, current. Molecular-dynamic calculations were performed with the following parameters: simulation time, 10 ps; step width, 1 fs; temp., 300 K; constant temperature with 10 fs relaxation time; snapshot interval 10 fs. MULTIFIT Procedure [34]: spring constant 20 kcal/mol · Å^2.

4. Results. – Three pharmacophoric (osmophoric) points of sandalwood-odor molecules were assumed: the OH group (P1) as most reactive group of the molecule, with the possibilities to build a H-bond to the receptor protein, a lipophilic group (P2) in the

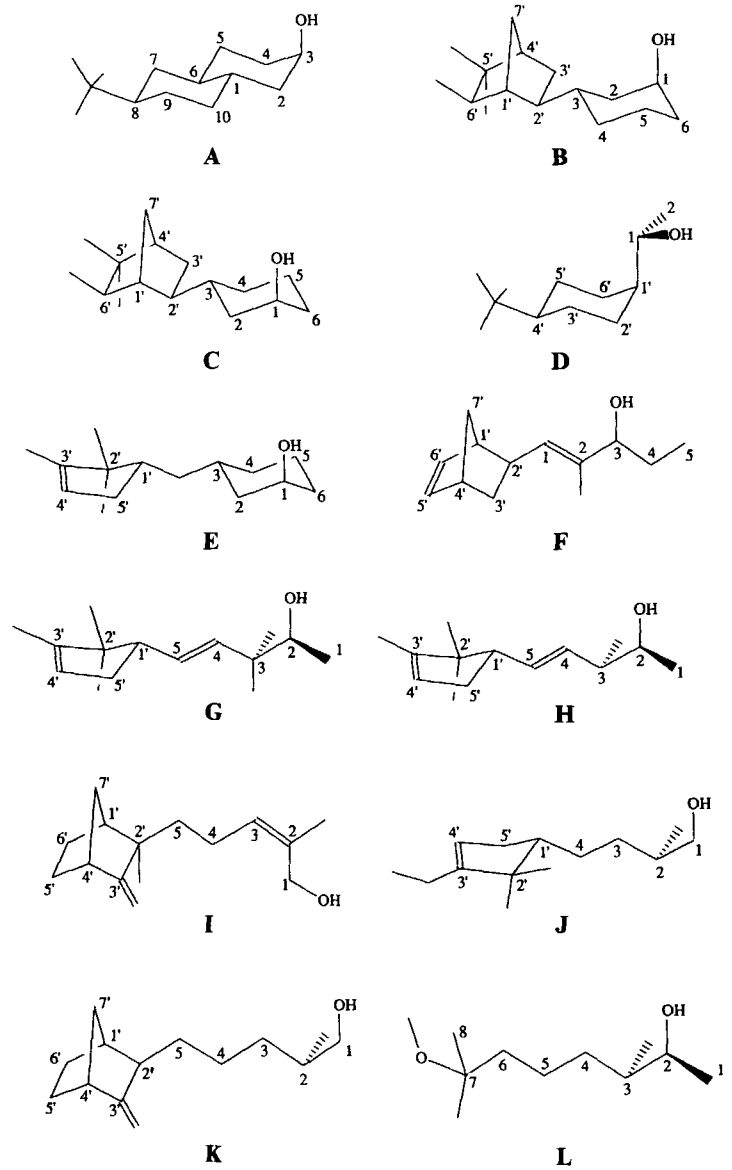

Fig. 1. *Sandalwood-odor molecules used for the 'active-analog approach'*. **A**, 6α-(*tert*-Butyl)-*trans*-perhydronaphthalen-2α-ol [17] [18]; **B**, (1*RS*,3*RS*,1′*SR*,2′*RS*,4′*SR*,6′*SR*)-3-(5′,5′,6′-trimethylbicyclo[2.2.1]hept-2′-yl)cyclohexan-1-ol [19]; **C**, (1*RS*,3*RS*,1′*RS*,2′*SR*,4′*RS*,6′*RS*)-3-(5′,5′,6′-trimethylbicyclo[2.2.1]hept-2′-yl)cyclohexan-1-ol [19]; **D**, 1-[4-(*tert*-butyl)cyclohexyl]ethanol [20] [21]; **E**, 3-(2′,2′,3′-trimethylcyclopent-3′-enyl)cyclohexan-1-ol [22]; **F**, 1-(bicyclo[2.2.1]hept-5′-en-2′yl)-2-methylpent-1-en-3-ol [23]; **G**, 3,3-dimethyl-5-(2′,2′,3′-trimethylcyclopent-3′-enyl)pent-4-en-2-ol [24]; **H**, 3-methyl-5-(2′,2′,3′-trimethylcyclopent-3′-enyl)pent-4-en-2-ol [25]; **I**, 2-methyl-5-(2′-methyl-3′-methylidenebicyclo[2.2.1]hept-2′-yl)pent-2-en-1-ol [26]; **J**, 4-(3′-ethyl-2′,2′-dimethylcyclopent-3′-enyl)-2-methylbutan-1-ol [27]; **K**, 2-methyl-5-(3′-methylidenebicyclo[2.2.1]hept-2′yl)pentan-1-ol [28]; **L**, 3,7-dimethyl-7-methoxyoctan-2-ol [29].

neighborhood of the OH group, and a part of the bulky aliphatic group (P3). First the osmophoric points in compound **A** were defined, namely the O-atom (P1), the C-atom connected with the O-atom (C(3), see *Fig. 1*; P2), and the atom C(8), to which the *t*-Bu group is bound (P3). To obtain some information about the variability of the distances between the osmophoric points caused by the internal motion of the molecule, molecular-dynamic experiments were performed yielding an estimation of the deviations from the energy minimum of compound **A**. The results of this analysis are listed *Table 1*.

Table 1. *Internal Movement of the Defined Osmophoric Points of* **A** *by Molecular Dynamics* (distances in Å). The first pharmacophoric point is the O-atom of the OH group.

	Maximum distance	Minimum distance	Average distance
O–C(8)	6.21	5.37	5.76
C(3)–C(8)	5.59	5.18	5.39

Although molecule **A** seems to be rather rigid and exists only in one conformation, deviations for the postulated osmophoric pattern of *ca.* 0.4 Å were observed. Using systematic SEARCH with distance map constraints, a determination of common orientations of the osmophoric points in all mentioned sandalwood-odor molecules was done. The 'active-analog approach' failed. Due to the high number of possible conformations, no significant osmophoric pattern could be found. Additionally, the distance between P1 and P2 appeared to be too short for a concise analysis for all investigated compounds.

To avoid these limitations, the more flexible molecule **E** [22] was selected as starting compound for the approach. All sterically and energetically allowed conformations for compound **E** were calculated (*Table 2*). A distance map of the unconstrained osmophoric orientations of compound **E** (distances P1–P2, P1–P3, and P2–P3) was generated and the

Table 2. *Osmophoric Points P2 and P3 of Compounds* **E**–**L**, *Compared to the Number of Single Bonds Between the Pharmacophoric Points and the Resulting Number of Possible and Active Conformations*

	Osmophoric point P2	Osmophoric point P3	Number of rotating single bonds	Number of possible conformations	Number of active conformations
E	C(5) in the cyclohexane ring	dummy atom as center of the cyclopentene ring	2	100	2
F	C(5) in the side chain	dummy atom as center of the norbornane bicycle	3	5	2
G	C of Me at C(3)	dummy atom as center of the cyclopentene ring	3	27	14
H	C of Me at C(3)	dummy atom as center of the cyclopentene ring	3	18	8
I	C of Me at C(2)	dummy atom as center of the norbornane bicycle	4	2	2
J	C of Me at C(2)	dummy atom as center of the cyclopentene ring	4	26	26
K	C of Me at C(2)	dummy atom as center of the norbornane bicycle	5	49	49
L	C of Me at C(3)	quarternary C(7)	5	162	162

obtained information transferred to the more flexible compound **F** and so on. Additionally, the osmophoric point P3 was assumed in some cases as a 'dummy atom' [15] in the center of a ring system. In *Table 2*, the definition of the osmophoric points for all flexible compounds are listed together with the results of the systematic search. The dummy atoms mentioned in *Table 2* were constructed as centroids of the seven atoms of the norbornane (8,9,10-trinorbornane) ring system or of the five atoms of the cyclopentene ring.

From the 100 energetically possible conformations of **E**, 63 different osmophoric orientations were found at the beginning of the approach. The application of the calculated distance map and the connected conformational search on compound **F** led to only 5 conformations for his more flexible molecule. These conformations showed 4 different orientations of the osmophoric points. Recalculation of the distance map and its application to the next compound **G** and subsequently **H** produced 27 and 18 possible conformations, respectively. Again, 4 different orientations of the osmophoric points were possible. The same procedure for compound **I**, led to only 2 conformations, both with different osmophoric orientations. The 'active-analog approach' for **J**, **K**, and the extreme flexible molecule **L** produced 26, 49, and 162 conformations, respectively, according to the distance map containing two orientations. For the estimation of the active conformations of compounds **E**–**H**, the whole procedure was repeated with the restricted osmophoric pattern. The number of conformations which were in agreement with both osmophoric models for compounds **E**–**L** are shown in the last column of *Table 2*.

Table 3 shows the distances of the osmophoric points (P1–P2, P1–P3, P2–P3), evaluated from compounds **E**–**L** by the 'active-analog approach'. The accuracy of the distances (0.1 Å) is a consequence of the grid-size value of the SEARCH program. The differences between both osmophoric models were not very large. In *Fig. 2*, the two orientations are visualized. The axes in the orientation space map represent the distances between two of three osmophoric points. Each osmophoric model is, therefore, given as a triangle in the three-dimensional graph. As the distance P1–P2 was identical in both models, the triangles are located in a plane perpendicular to the P1–P2 axis.

Table 3. *Distances of the Osmophoric Points Evaluated by the Comparison of Compounds* **E**–**L** *for the Two Obtained Orientations*

	Distance P1–P2 [Å]	Distance P1–P3 [Å]	Distance P2–P3 [Å]
Orientation 1	2.9–3.0	6.2–6.3	5.6–5.7
Orientation 2	2.9–3.0	6.3–6.4	5.9–6.0

To obtain more detailed information about both orientations, a MULTIFIT calculation was performed. The lowest-energy conformation of the active conformations (*Table 2*) of each compound **E**–**L** was selected. These eight conformations were linked together with the coincidence of the individual osmophoric points P1, P2, and P3. The geometry of the resulting 'supermolecule' was minimized simultaneously with the minimization of the distances between the individual osmophoric points (P1–P1′–P1″–..., P2–P2′–P2″..., ...), applying the sum of the square distances with a spring constant of 20 kcal/mol · Å^2. This procedure was performed with both osmophoric orientations as starting conformations. In *Tables 4* and *5*, these energies are listed together with the energy differences to the

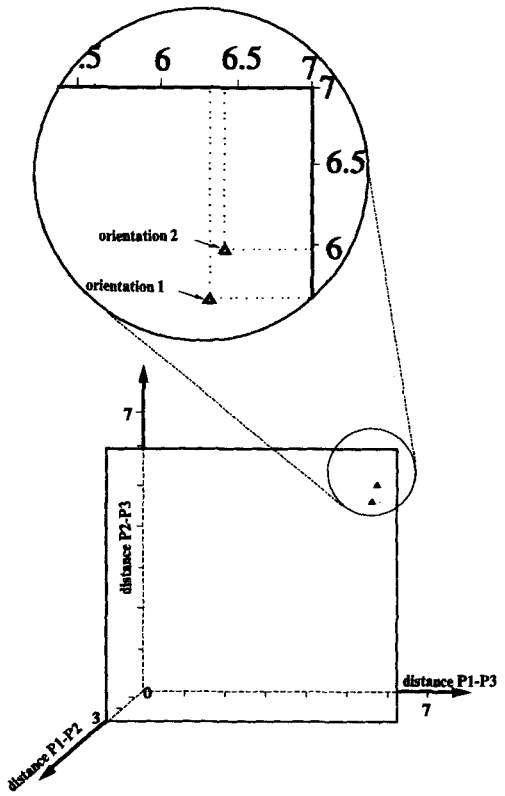

Fig. 2. *Three-dimensional orientation space map for the molecules* **E**–**L**. The axes represent the distance between two of the three osmophoric points.

absolute energy minima of each compound. As shown in both tables, the RMS values (root-mean-square values) indicate a good matching of all conformations to the osmophoric models, described by molecule **E** as reference. Nevertheless, the fitting procedure to orientation 2 seems to be more convenient because in the average as well as for the maximum values, the energy differences to the corresponding total minima were less than for orientation 1.

Table 4. *MULTIFIT Fitting Procedure on the Minimized Sandalwood-Odor Molecules* **E**–**L** *with the Osmophoric Model 1.* Distances P1–P2 = 2.95, P1–P3 = 6.25, and P2–P3 = 5.65 Å.

	MULTIFIT Energy [kcal/mol]	Total minimum energy [kcal/mol]	Energy difference [kcal/mol]	RMS Value
E	8.81	8.56	0.25	0.000
F	26.86	24.51	2.35	0.009
G	9.99	8.39	1.60	0.016
H	10.19	6.48	3.71	0.017
I	26.15	22.86	3.29	0.015
J	11.69	9.27	2.42	0.010
K	23.80	20.85	2.95	0.016
L	10.46	6.19	4.27	0.027

Table 5. *MULTIFIT Fitting Procedure on the Minimized Sandalwood-Odor Molecules* **E–L** *with the Osmophoric Model 2.* Distances P1–P2 = 2.95, P1–P3 = 6.35, and P2–P3 = 5.95 Å.

	MULTIFIT Energy [kcal/mol]	Total minimum energy [kcal/mol]	Energy difference [kcal/mol]	RMS Value
E	10.30	8.56	1.74	0.000
F	25.73	24.51	1.22	0.022
G	9.25	8.39	0.86	0.022
H	6.50	6.48	0.02	0.009
I	25.07	22.86	2.21	0.006
J	11.82	9.27	2.55	0.032
K	24.19	20.85	3.34	0.017
L	9.09	6.19	2.90	0.017

Additionally the comparison of compounds **A–D** with both osmophoric patterns led to a better approximation for orientation 2 as examplified by the RMS values of a least-square fit of **A–D** to the osmophoric model (0.287 for orientation 1 and 0.208 for orientation 2). A matching for these rigid compounds to the osmophoric points was possible taking a tolerance distance between points P1, P2, and P3 to the defined centers in the rigid molecules of *ca.* 0.4 Å into account. This value also appeared in the molecular-dynamics analysis of compound **A**. From both studies (MULTIFIT procedure and comparison of the model with the rigid compounds **A–D**), orientation 2 was postulated to be more significant for the model, which explains the molecular substructure responsible for the biological effect, the sandalwood odor.

In *Figs. 3* and *4*, the osmophoric model is presented as a result of the 'active-analog approach'. The MULTIFIT procedure for orientation 2 led to the superposition of molecules **E–L** (*Fig. 3a*). Additionally, the rigid compounds **A–D**, which were fitted to the osmophoric pattern are included in *Fig. 3b*. The green bulks represent the osmophoric points of the sandalwood-odor activity: the larger bulk on the left side correlates to P3, the center of the aliphatic residues. P1 appears at the top of the right side, and P2 is the green bulk below P1. The shape of the bulks was estimated from the common molecular volumes of the osmophoric patterns of all fitted molecules. The osmophoric points P1, P2, and P3 for the fitting procedure of molecules **A–D** to the osmophoric pattern of compounds **E–L** are given in *Table 6*. The three osmophoric points in compounds **A** and **I** as representatives of enantiomerically pure sandalwood-odor molecules are shown in *Fig. 3c*. The molecular surface of *Fig. 4* is the envelope over all superpositioned compounds **A–L**. As these substances (**A–L**) are representative for a large number of sandalwood-odor molecules, the osmophoric points on this surface should be valid generally for sandalwood-odor molecules.

To prove the model of the osmophoric pattern of the sandalwood-odor, some structurally similar, but odorless compounds were compared with the 'average sandalwood molecule'. In *Fig. 5* the structure of these odorless test compounds are shown. Compounds **a** and **b** are isomers of **B** and **C** and are described as racemates [19]. Compound **c** is a truncated structural analogue of substance **D** without the α-positioned Me group. The differences between **d**, **e**, and **H** is only the configuration at C(2) and C(3). Compound **f** is similar to **E** with an elongation of the C-chain between the two cyclic systems. For these compounds, the various isomers were compared, and again the structure was considered which showed the best agreement with the standard sandalwood

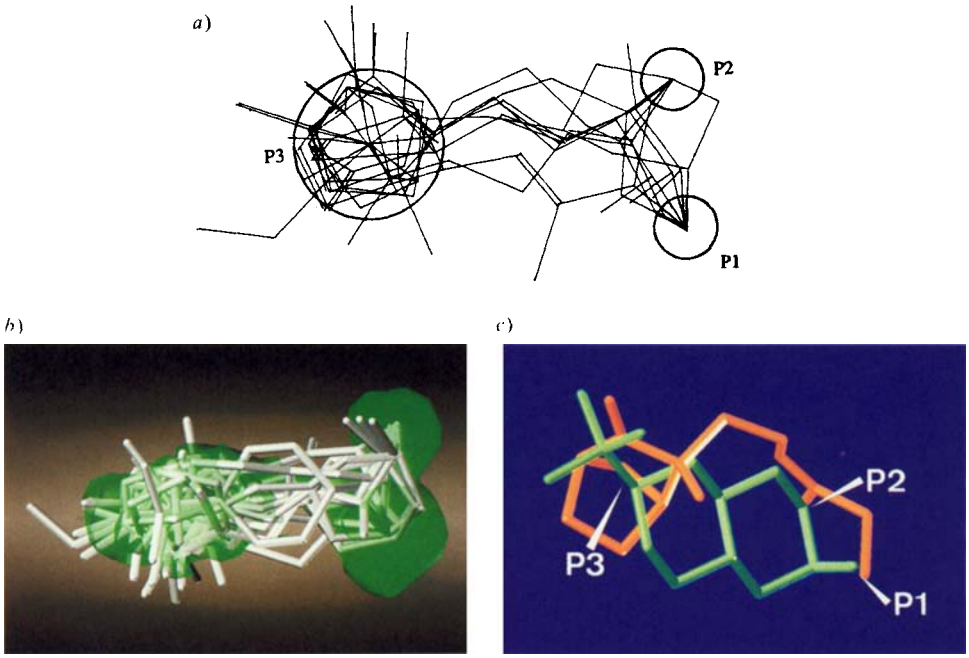

Fig. 3. a) *Superimposed molecules* **E**–**L** *as the result of the simultaneous minimization* (the circles indicate the three osmophoric groups P1, P2, and P3), b) *superpositioned molecules* **A**–**L** *together with the osmophoric model* (green; only the heavy-atom skeletons of the molecules are shown), *and* c) *superimposed molecules* **A** (green) *and* **I** (orange) *with the pharmacophoric points P1, P2, and P3*

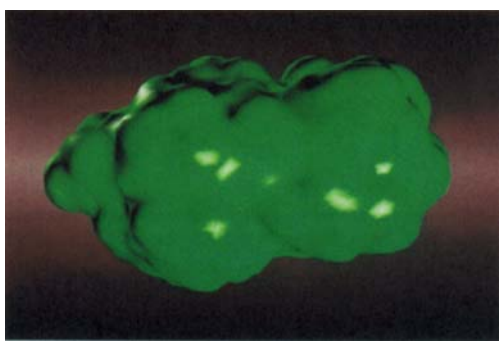

Fig. 4. *Molecular surface of the 'supermolecule', constructed from the superposition of molecules* **A**–**L**

Table 6. *Osmophoric Points P1, P2, and P3 of Molecules* **A**–**D** *for the Fitting Procedure to the Osmophoric Pattern of Compounds* **E**–**L**

	Osmophoric point P1	Osmophoric point P2	Osmophoric point P3
A	*OH*	C(4) in the decalin ring	C(8)
B	*OH*	C(5) in the cyclohexane ring	dummy atom as center of the norbornane bicycle
C	*OH*	C(5) in the cyclohexane ring	dummy atom as center of the norbornane bicycle
D	*OH*	C(2) (Me group)	quaternary C of *t*-Bu

molecule **A**. The odorless compounds were fitted to the osmophoric model in analogy to the procedure for the odor compounds **A**–**L**. Some conformations were found which followed exactly the distance matrix, but in contrary to the odor compounds, these substances showed deviations of the molecular surface in the region of the osmophoric points. Compound **c**, the chain-truncated analogue of **D**, is odorless, which can be explained by the lack of the osmophoric point P2 – the Me group (C(2)) in **D**. An exception is compound **f**, which can be fitted in agreement with the model. Therefore, the lack of sandalwood odor cannot be explained by molecular-shape comparison in this manner. Probably, physicochemical reasons – *e.g.* an insufficient vapor pressure – are responsible for the odor property.

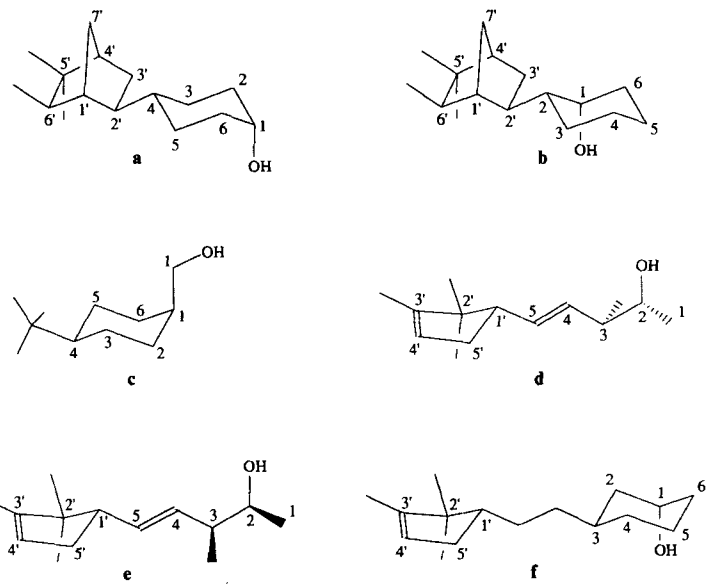

Fig. 5. *Molecules with structural similarity to sandalwood-odor compounds, but without odor.* **a**, 4-(5′,5′,6′-Trimethylbicyclo[2.2.1]hept-2′-yl)cyclohexan-1-ol [19]; **b**, 2-(5′,5′,6′-trimethylbicyclo[2.2.1]hept-2′-yl)cyclohexan-1-ol [19]; **c**, 4-(*tert*-butyl)cyclohexane-1-methanol [34]; **d**, (1′*S*,2*R*,3*R*)-3-methyl-5-(2′,2′,3′-trimethylcyclopent-3′-enyl)pent-4-en-2-ol [21] [25]; **e**, (1′*S*,2*S*,3*S*)-3-methyl-5-(2′,2′,3′-trimethylcyclopent-3′-enyl)pent-4-en-2-ol [21] [25]; **f**, 3-[2-(2′,2′,3′-trimethylcyclopent-3′-enyl)ethyl]cyclohexanol [7].

A graphical presentation of the fitting of two odorless compounds is shown in *Fig. 6*: the cyan-colored odorless molecules were compared with the odor compounds (white). The yellow or green bulks represent the deviations of the molecular volume of the test compounds with the common volume of the superpositioned odor molecules. In case of compound **d** (*Fig. 6a*), pronounced deviations close to the osmophoric points P1 and P2 can be recognized. Compound **a** (*Fig. 6b*) shows a large bulky deviation at P3, at the aliphatic residue of the molecules. In both cases, the positive deviation from the ideal molecular surface at the region of the osmophoric points hinders an association to the corresponding receptor.

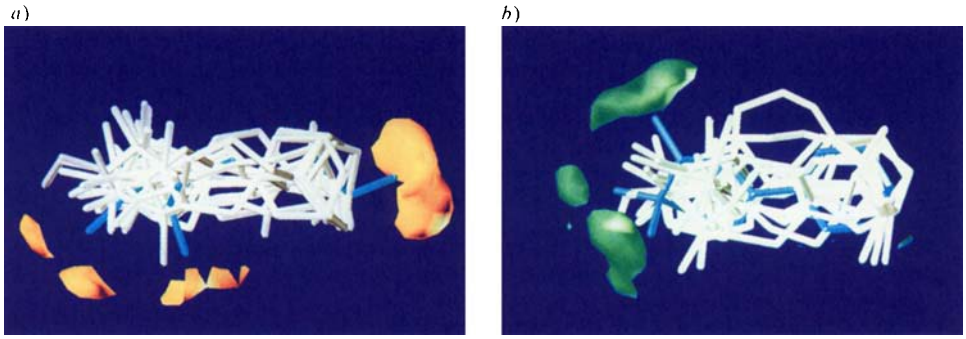

Fig. 6. a) *Comparison of the odorless compound* **d** (cyan) *with the odor compounds* **A**–**L** (white; the deviations from the common volume of the odor substances are shown as yellow bulks) *and* b) *comparison of the odorless compound* **a** (cyan) *with the odor compounds* **A**–**L** (white; the deviations from the common volume of the odor substances are shown as green bulks)

In *Fig. 7*, the deviations of all odorless compounds used as a prove of the osmophoric model are shown. The bulks of the deviation volumina are concentrated at the osmophoric points. The molecular surface of a sandalwood-odor molecule consists, therefore, of some regions which have to follow exactly the osmophoric model evaluated in this work, and of some less important parts where the molecular shape can vary to some extent. Only too large deviations may additionally hamper an association at the receptor site. Especially the osmophoric point P2 in the neighborhood of the OH group seems to be rather sensitive, as shown by the comparison of the odor compound **H** with its odorless isomers **d** and **e**. This feature was already postulated based on investigations of the odor differences between the optical isomers of **A** [14] [18]. Also, the comparison of substances **c** and **D** shows that a hydrophobic domain (*e.g.* a stereoselectively branched group) in α-position enhances/reinforces/strengthens the odor impression.

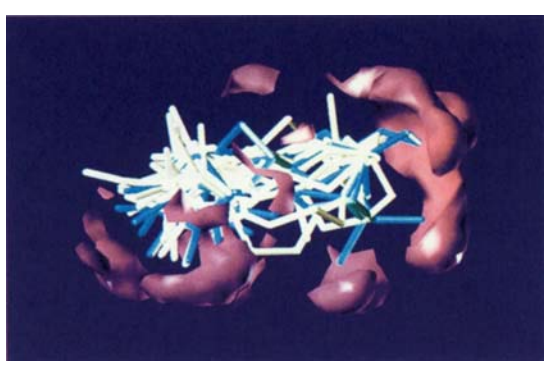

Fig. 7. *Comparison of the odorless compounds* **a**–**f** (cyan) *with the odor compounds* **A**–**L** (white). The sum of the deviations of all odorless compounds used in the calculations are shown by the violet bulks.

The authors would like to thank Dr. *Hecht* from *Sandoz*, Austria, for technical support, Prof. *Fleischhacker* for the disposal of the *Sun-Sparc* workstation, Dr. *Haider* and Dr. *Ecker* for their help, and Fa. *Dragoco*, Vienna, for its interest.

REFERENCES

[1] G. Buchbauer, A. Neumann, U. Siebenheitl, P. Weiss, P. Wolschann, *Monatsh. Chem.* **1994,** *125,* 747.
[2] G. R. Marschall, in '3D QSAR in Drug Design, Theory Methods, and Application', Ed. H. Kubinyi, ESCOM Science Publishers B. V., Leiden, 1993, p. 80.
[3] G. R. Marshall, C. D. Barry, H. E. Bosshard, R. A. Dammkoehler, D. A. Dunn, *ACS Symp. Ser.* **1979,** *112,* 205.
[4] E. J. Lloyd, P. R. Andrews, *J. Med. Chem.* **1986,** *29,* 453.
[5] R. A. Dammkoehler, St. F. Karasek, E. F. Berkley Shands, G. R. Marshall, *J. Comput.-Aided Mol. Design* **1989,** *3,* 3.
[6] D. Mayer, Ch. B. Naylor, I. Motoc, G. L. Marshall, *J. Comput.-Aided Mol. Design* **1987,** *1,* 3.
[7] E. J. Brunke, E. Klein, in 'Fragrance Chemistry – The Science of the Sense of Smell', Ed. E. T. Theimer, Academic Press, New York, 1982.
[8] M. Chastrette, D. Zakarya, C. Pierre, *Eur. J. Med. Chem.* **1990,** *25,* 433.
[9] G. Buchbauer, S. Winiwarter, P. Wolschann, *J. Comput.-Aided Mol. Design* **1992,** *6,* 583.
[10] A. Beyer, P. Wolschann, A. Becker, E. Pranka, G. Buchbauer, *Monatsh. Chem.* **1988,** *119,* 711.
[11] A. Becker, G. Buchbauer, S. Winiwarter, P. Wolschann, *Monatsh. Chem.* **1992,** *123,* 405.
[12] G. Buchbauer, K. Leonhardsberger, S. Winiwarter, P. Wolschann, *Helv. Chim. Acta* **1992,** *75,* 174.
[13] G. Buchbauer, A. Stock, P. Weiss, S. Winiwarter, P. Wolschann, *Z. Naturforsch., B* **1992,** *47,* 1759.
[14] A. Neumann, P. Weiss, P. Wolschann, *J. Mol. Struct.* **1993,** *296,* 145.
[15] A. Becker, G. Buchbauer, S. Winiwarter, P. Wolschann, *J. Ess. Oil Res.* **1990,** *2,* 221.
[16] B. Treitl, Diploma Thesis, University of Vienna, 1993.
[17] J. G. Witteveen, A. J. A. Van der Weerdt, *Recl. Trav. Chim. Pays-Bas* **1987,** *109,* 29.
[18] G. Buchbauer, H. Spreitzer, H. Swatonek, P. Wolschann, *Tetrahedron: Asymmetry* **1992,** *3,* 197.
[19] E. Demole, *Helv. Chim. Acta* **1969,** *52,* 2065.
[20] G. W. Shaffer, K. L. Purzycki, US Pat. 4181631 (1980); Dt. Pat. 2804075, 1978 (*CA:* **1978,** *89,* 1796081).
[21] R. E. Naipawer, ACS-Meeting Abstract 1988, September 25–30, Los Angeles.
[22] E. J. Brunke, E. Klein, Dtsch. Offenlegungsschrift 1979, 2935683 (*CA:* **1981,** 42484c).
[23] T. Kobayashi, H. Tsuruta, T. Yoshida, K. Yokohama, Dtsch. Offenlegungsschrift, 1979, 2833283 (*CA:* **1979,** *90,* 168153j).
[24] K. H. Schulte-Elte, B. Müller, H. Pamingle, Eur. Pat. 155591, 1985 (*CA:* **1986,** *105,* 191435g).
[25] R. E. Naipawer, Eur. Pat. 203528, 1986 (*CA:* **1987,** *106,* 175828k).
[26] A. Krotz, G. Helmchen, *Tetrahedron: Asymmetry* **1990,** *1,* 537.
[27] K. Schulze, K. Beutmann, A.-K. Habermann, U. Himmelreich, *J. Prakt. Chem.* **1993,** *335,* 445.
[28] H. C. Kretschmar, W. F. Erman, US Pat. 3673261, 1972 (*CA:* **1972,** *77,* 113906h).
[29] B. N. Jones, H. R. Ansari, B. G. Jaggers, J. F. Jones, Dtsch. Offenlegungsschrift, 1973, 2255199 (*CA:* **1973,** *79,* 41918e).
[30] 'SYBYL, Molecular Modeling System, Version 6.0', Tripos Associates, Inc. St. Louis, MO.
[31] G. Chang, W. C. Guida, W. C. Still, *J. Am. Chem. Soc.* **1989,** *111,* 4379.
[32] I. Motoc, R. A. Dammkoehler, D. Mayer, J. Labanowski, *Quant. Struct.-Act. Relat.* **1986,** *5,* 99.
[33] N. L. Allinger, U. Burkert, 'Molecular Mechanics', ACS Monograph No. 177, Am. Chem. Soc. Washington D.C., 1982.
[34] J. Labanowski, I. Motoc, Ch. B. Naylor, D. Mayer, R. A. Dammkoehler, *Quant. Struct.-Act. Relat.* **1986,** *5,* 138.